Desalination and Water Treatment
www.deswater.com

doi: 10.5004/dwt.2017.20999

80 (2017) 344–351
June

Nitrate removal from aqueous solution by almond shells activated with magnetic nanoparticles

Mohsen Arbabi[a], Sara Hemati[a,*], Zahra Shamsizadeh[b], Arman Arbabi[c]

[a]*Department of Environmental Health Engineering, School of Health, Shahrekord University of Medical Sciences, Shahrekord, Iran, Tel. +98 38 33333710; Fax: +98 38 33334678; emails: hemati.sara88@yahoo.com (S. Hemati), marbabi47@yahoo.com (M. Arbabi)*
[b]*Environmental Science and Technology Research Center, Department of Environmental Health Engineering, Shahid Sadoughi University of Medical Sciences, Yazd, Iran, email: z_shamsizadeh69@yahoo.com*
[c]*Department of Environmental Health Engineering, School of Health, Shahid Beheshti University of Medical Sciences, Tehran, Iran, email: armanarbabi@gmail.com*

Received 25 November 2016; Accepted 4 June 2017

ABSTRACT

Magnetic activated carbons from almond shells were prepared, characterized, and used to remove nitrate from aqueous environments. The magnetic carbon was prepared by mixing of activated carbon in aqueous suspensions with an aqueous Fe^{3+}/Fe^{2+} solution followed by treatment with sodium hydroxide. The morphologies and surface chemistries of magnetic activated carbon were studied by Fourier transform infrared spectroscopy, field emission scanning electron microscopy, energy dispersive X-ray microanalysis, pH_{pzc}, and Brunauer–Emmett–Teller (BET) analyses. The BET area of magnetic activated carbon was 105.480 m^2/g. The effects of adsorbent dosage, the pH of the solution, initial nitrate ion concentration, and contact time on the removal process were investigated. The amount of remaining nitrate ion was measured by spectrophotometer UV–Vis after filtration. At optimum pH of 4 and equilibrium time of 20 min, adsorption efficiency increased with both increasing of absorbent concentration to 1 g/L and reduction of initial concentration of nitrate ions (76.29%). The equilibrium adsorption was best described by the Langmuir isotherm model ($R^2 = 0.924$). The almond shell activated with magnetic nanoparticles has a good ability to remove nitrate ions from aqueous solutions. Therefore, the use of this relatively easy and simple technology is an effective step in removing nitrate from water.

Keywords: Adsorption; Activated carbon; Almond; Magnetite nanoparticles; Nitrate

1. Introduction

One of the most important environmental problems in some regions of the world is contamination of underground waters by nitrate. Currently, nitrate is known as one of the world's most common chemical pollutants. Indiscriminate use of chemical fertilizers in agriculture, population growth, over-harvesting of groundwater aquifers and industry growth have led to increase in nitrate concentrations in groundwater [1,2]. Water sources have been highly polluted with nitrogenous compounds such as nitrate, nitrite, and ammonium, which could result in severe environmental problems including eutrophication and infectious diseases. Increased nitrate concentrations in drinking water may lead to diseases such as methemoglobin in children, gastric cancer, miscarriage, and hypertension and thyroid disorders [3,4].

Nitrate ion is relatively non-toxic, but when reduced to nitrite, it endangers public health. Nitrite is combined with hemoglobin in infants, younger than 6 months, and produces methemoglobin, which is unable to transport oxygen to the tissues and causes the blue color of the blood. This condition is known as blue baby syndrome [1,5]. Nitrates may also react with second and third type amines and forms a carcinogenic form [6]. According to the US Environmental Protection Agency (EPA) and the World Health Organization (WHO)

* Corresponding author.

guidelines, the maximum allowable concentration of nitrate is 10 mg/L as nitrogen and 50 mg/L as nitrate for public water supply system [7].

The Iran Regulations of Quality (Standard No. 1053) authorized limit for nitrate in drinking water is 50 mg/L [8]. Several methods have been reported for nitrate removal from water, in which most common are biological, chemical, and physical processes [9]. The most important, acceptable technique to treat the high concentrations of nitrate is use of biological reactors; therefore, it is done mainly for sewage treatment and is not desired for water treatment due to organic substrates as well as the need for careful maintenance [3]. Conventional physical and chemical processes for the removal of nitrate are ion exchange, reverse osmosis, electrodialysis, chemical reduction, and surface adsorption [9].

All the above techniques, in addition to adverse effects on water, require a large initial investment, high operational and utilization costs, and even lead to producing secondary contaminated effluent and are not economically viable at large scale [3,10]. Today, the use of nanotechnology and adsorption process for the removal of some contaminants such as nitrate ions from water is increasing [5,11]. Use of coconut and almond shells, sugar beet and bagasse and wheat husk for nitrate removal from aqueous solutions has been of great interest to researchers as these are inexpensive and natural absorbents [11]. Adsorption is a suitable method of choice to remove some contaminants such as nitrate because of the simplicity of design, material cost, ease of removal, and no need for final treatment [12].

Due to growth of agricultural and industrial activities in the last decade, leading to increased disposal of treated and untreated wastewater to the environment, nitrate concentrations in groundwater resources have exceeded in many urban and rural areas [13,14]. Unfortunately, the main problem in the use of activated carbon powder or the absorbents with nanosize or nanoparticles is their separation from the solution due to the small size of particles. Thus, the distribution and production of secondary pollution are the fundamental problems of these systems [15,16].

Magnetic nanoparticles have been of great interest to researchers due to unique magnetic properties [17]. Therefore, these absorbents' magnetism could be an appropriate strategy to eliminate many of these problems [18].

According to the conducted studies, almond shell charcoal and magnetic nanoparticles have very good ability to remove organic compounds and toxic heavy metals from aqueous solutions [14,18,19]. Almond is abundantly produced and harvested in Iran. For this reason, the use of activated carbon made from almond shell as an absorbent is justifiable due to low price, large quantity available, and simple preparation and operation [20]. Therefore, this study is conducted to investigate the use of the processed carbon absorbent activated with iron nanoparticles from almond shell to remove nitrate in aqueous environments.

2. Materials and methods

In this experimental study, the use of almond shell activated with magnetic nanoparticles to remove nitrate in aqueous environments was investigated.

2.1. Absorbent preparation

The type of almond used was Mamaei almond purchased from the stores in Shahrekord, Chaharmahal-o-Bakhtiari. After being separated and washed with distilled water, almond shell was ground using grinding mill. The ground samples were placed in phosphoric acid at room temperature and 1:1 ratio with weight percentage of 50% for 24 h to reduce alkaline property and to eliminate impurities (such as calcium carbonate). Then, they were rinsed twice with distilled water and dried in an oven at 100°C for 24 h [20–22]. For heating activation, samples were placed in an oven at 700°C for 1 h [23]. So that, in this case, the adsorption and absorbent porosity increased greatly. The activated sample was pulverized in a porcelain mortar and passed through a sieve with standard mesh 30 (500 μm) and 100 (150 μm) so that a uniform powder was obtained [22].

2.2. Activation of absorbent with iron magnetic nanoparticles

Activated carbon (50 g) was mixed with 500 mL of distilled water. To prepare ferric chloride ($FeCl_3 \geq 96\%$) solution, 18 g of ferric chloride was mixed with 1,300 mL of distilled water (it should be prepared at the time of testing). To prepare ferrous sulfate ($FeSO_4$, 99.5%) solution, 20 g of ferrous sulfate was mixed with 150 mL of distilled water. Then, ferric chloride and ferrous sulfate solutions were mixed together and stirred at a temperature of 60°C–70°C very quickly. The solution obtained was combined with a solution of activated carbon and gently stirred at room temperature for 30 min. The solution of 10 M sodium hydroxide (NaOH) was added to the suspension drop by drop until the pH reached 10–11. After 60 min of stirring, the suspension was maintained for 24 h at room temperature and then washed several times with distilled water and then with ethanol. The obtained suspension was vacuum-filtered and dried overnight in an oven at 50°C. Hence, the activated carbon with magnetic nanoparticles was prepared [18,24]. All chemicals used in the preparation of nanoparticles were purchased from Merck & Co., Germany.

2.3. Measurement of zero point charge

For measurement of zero point charge (pH_{pzc}) of the magnetic activated carbons, 100 mL of nitrate solution with concentration of 25 mg/L was used. pH_{pzc} was measured using normal sulfuric acid 0.1 and/or normal sodium hydroxide 0.1 at pH 2, 4, 6, 8, and 0.5 g/mL where magnetic activated almond shell was added to each solution and was stirred for 24 h. The supernatant was then decanted and its pH was measured using digital pH meter (METTLER, model Mp230). The curve of initial pH vs. secondary pH was drawn and confluence point of two curves was presented as isothermic pH point [18].

2. 4. Experimental design

All experiments were performed in a batch reactor (flask). To prepare a solution of water and nitrate at concentrations of interest, we used its mineral resource, namely potassium nitrate.

The 100 mL of initial nitrate standard solutions (25, 50, 100, 200, and 400 mg/L) was poured into 250 mL flask and a determined amount of magnetic nanoparticles activated absorbent (0.25, 0.3, 0.4, 0.5, and 1 g/L) was added to it. Sample pH values were adjusted by adding a few drops of normal sulfuric acid 0.1 and/or normal sodium hydroxide 0.1 at 4, 5, 6, 7, and 8 values using digital pH meter (METTLER, model Mp230) [4,18]. These experiments were done at 120 rpm mixer speed and detention time of 20, 40, 60, 80, and 100 min. Then, for absorbent separation, solutions were passed through 0.45-μm cellulose-acetate filter paper. The filtered solution was poured into the sampling containers (Falcon PVC), which were previously washed with ultrapure water and within less than 24 h, the absorbance of samples was read by a spectrophotometer (model UV-2100) at 296-nm wavelength [25].

The amount of absorbed nitrate was calculated from difference between the initial concentration of nitrate and the concentration after contact with absorbent. The obtained equilibrium concentrations were used to calculate the equilibrium capacity of nitrate ion adsorption per Eq. (1) [9,25]:

$$q = \frac{\left(C_0 - C_e\right) \times V}{M} \tag{1}$$

where C_e (mg/L), the equilibrium concentration of absorbate; C_0 (mg/L), the initial concentration; V (L), the solution volume; and M (g), absorbent mass.

The prepared absorbent was characterized by Brunauer–Emmett–Teller (BET) experiment. For determination of functional groups of synthesized absorbent, Fourier transform infrared spectroscopy (FTIR) was used. In addition, morphology, shape, and particle size distribution of the microstructures were checked in the images taken by field emission scanning electron microscopy (FESEM) [18,21].

In this study, the experiments were designed and the data were analyzed by response surface method, statistical modeling method of full factorial design was done by Design Expert version 07, and one-way analysis of variance (ANOVA) was used for results interpretation. P value <0.05 was considered as the level of significance. In this study, pH, contact time, and adsorbent dose were considered as independent variables and nitrate removal efficiency as response variable.

3. Results and discussion

3.1. Absorbents characteristics

The results of BET experiment are shown in Table 1. Functional groups of absorbent formation per FTIR analysis are shown in Fig. 1.

Fig. 1 illustrates the FTIR spectrum of almond coal activated with magnetic nanoparticles. The observed peak at 3,179 cm^{-1} wavelength was obtained for the OH functional group on the surface of iron particles. At 1,699 and 1,133 cm^{-1} wavelengths, functional groups of carbonyl C=O and ester C–O, respectively, are seen. The observed peaks at 473, 739, and 1027 cm^{-1} wavelengths were obtained for silicate phases. In addition, the observed peak at 584 cm^{-1} wavelength was obtained for iron bonds Fe–O.

Table 1
Results of BET experiment

Type of absorbents	Specific surface area (m^2/g)
Almond shell carbon	54.254
Almond shell carbon activated with magnetic nanoparticles	105.480

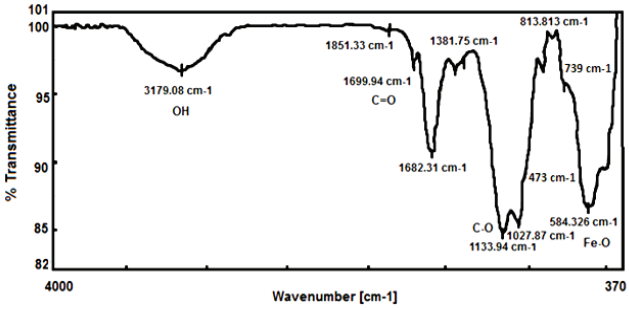

Fig. 1. FTIR result of activated almond shell carbon.

Both FESEM and energy dispersive X-ray microanalysis (EDX) images of synthesized absorbent are shown in Figs. 2 and 3. By the analyses, the main elements of synthesized absorbent are carbon, oxygen, and iron (Table 2). The size of synthesized absorbent is illustrated in Fig. 2(a). Fig. 2(b) depicts the nanometry particles in the absorbent. Besides them, large and blade particles can be seen as well, probably related to the carbon particles of the almond shell.

3.2. Statistical analysis

As mentioned, in this study, method of full factorial design and one-way ANOVA were used for results interpretation of independent variables effects on response variable (nitrate removal efficiency). In Table 3 independent variables are depicted.

According to P values (Table 4), the effect and coefficients obtained for each factor, the regression equation of nitrate ion adsorption was obtained as Eq. (2). As P value is less than 0.05, so the studied model is significant.

$$\begin{aligned} Y = {} & 43.92 + 7.08A_1 + 2.57A_2 + 0.44A_3 - 3.05A_4 + 0.72B_1 + 0.19B_2 \\ & + 0.58B_3 - 1.35B_4 - 1.48C_1 + 1.49C_2 + 0.69C_3 + 1.96C_4 + 26.05D_1 \\ & + 10.94D_2 - 4.53D_3 - 9.58D_4 \end{aligned} \tag{2}$$

3.3. Effect of contact time

The effect of contact time on nitrate removal efficiency is shown in Fig. 4. According to this figure the most nitrate removal efficiency was obtained at first 20 min and it is equal to 76.29%.

Removal efficiency reaches an almost constant trend after 20 min, which could be considered the equilibrium retention time. Since giving further time to the system for adsorption after the actual time leads to no positive changes in nitrate adsorption efficiency; thus, 20 min could be considered as

optimal contact time. Janos et al. [26] showed that nitrate adsorption in the initial minutes occurred at high speed and then declined over time. In the study by Bhatnagar et al. [10], the maximum nitrate removal was achieved in the first 15 min of contact time. Ozmen et al. [27], regarding the removal of metal ions from aqueous solution using magnetite nanoparticles, concluded that very fast rate of adsorption and equilibrium adsorption can be achieved for all metals within few minutes. They attributed fast equalization within a short time to lack of resistance to internal diffusion. According to Li et al. [28], the maximum nitrate removal was achieved in initial contact time.

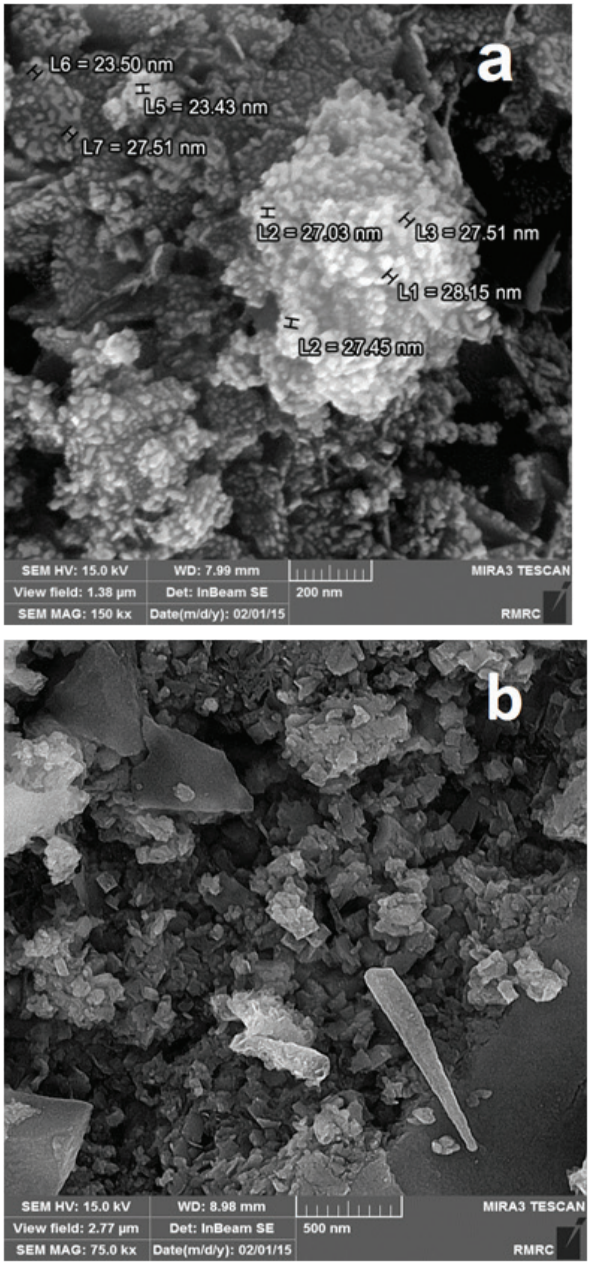

Fig. 2. FESEM images from almond shell carbon activated with magnetic nanoparticles: (a) size of synthesized absorbent and (b) nanometry particles in the absorbent.

3.4. Determining of optimum pH

Fig. 5 shows nitrate removal efficiency by changing the initial pH. As it is understood from this figure, by increasing the pH from 4 to 8, the removal efficiency of nitrate from 75.57% to 61.44% decreased and pH value of 4 was determined as an optimal pH.

In the present study, pH was demonstrated to highly contribute to achieving the maximum removal rate. As such, the efficiency of nitrate removal is maximal at pH 4. Linearly, with increase in pH, the efficiency of nitrate removal decreases. The increase in H^+ ions in the environment and decrease in OH^- ions could be the reason for increase in nitrate removal at pH 4. The adsorption rates of anions are higher at low pH and in the presence of H^+ ions. The reason for decreased efficiency of nitrate adsorption in alkaline pH is due to the increasing concentration of hydroxide ion in the solution and its replacement with nitrate ion at surface adsorption sites [29]. Our findings are consistent with Bhatnagar et al. [10].

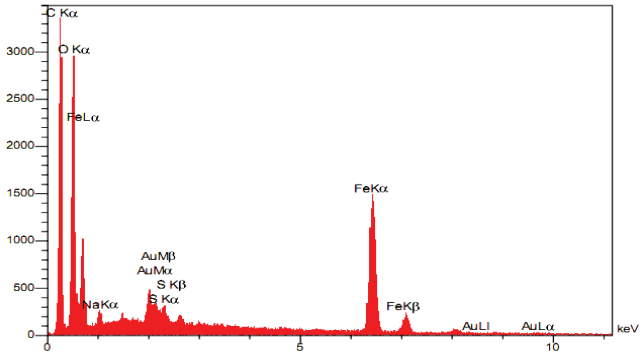

Fig. 3. EDX micrograph of almond shell carbon activated with magnetic nanoparticles.

Table 2
Percentage of main elements of synthesized absorbent

Elements	Weight percentage (%)
C	44.42
O	32.77
Na	0.7
S	0.64
Fe	19.66

Table 3
Levels and values of independent variables

Variables	Symbols	Agent levels				
		1	2	3	4	5
pH	A	4	5	6	7	8
Contact time (min)	B	20	40	60	80	100
Absorbent dose (g/L)	C	0.25	0.3	0.4	0.5	1
Initial concentration of NO_3 (mg/L)	D	25	50	100	200	400

Table 4
Analysis of variance for nitrate adsorption (classical sum of squares – Type II)

Source	Sum of squares	Df	Mean square	*F* value	*P* value
Model	60,188.78	16	3,761.80	42.68	<0.0001
A, pH	4,323.28	4	1,080.82	12.26	<0.0001
B, Time	105.81	4	26.45	0.30	0.8776
C, Absorbent concentration	457.81	4	114.45	1.30	0.2725
D, NO_3 concentration	54,353.21	4	13,588.30	154.16	<0.0001
Residual	15,248.48	173	88.14	–	–
Corrected total	75,437.26	189	–	–	–

Demiral et al. [4] studied the removal of nitrate from aqueous solution by activated carbon, and maximum nitrate removal (41.2%) was obtained at pH 3. According to Chatterjee et al. [5] the highest nitrate removal efficiency of 99% was observed at pH 5.6.

In the study by Hamoudi et al. [30], the optimal pH for nitrate adsorption was derived 6, which is much higher compared with the activated almond carbon.

The result of present study is similar with that of research conducted by Liou et al. [31], their study showed that at pH 4, nitrate removal by zerovalent iron nanoparticles reached 95%.

pH_{zpc} determines the type of absorbent surface charge. At the pH level of less than pH_{zpc}, absorbent surface charge is positive and at pH higher than pH_{zpc}, adsorbent surface charge is negative (Fig. 6).

3.5. Determining of optimum absorbent dose

The effect of initial dose of adsorbent on nitrate removal efficiency was investigated by changing the initial dose of adsorbent (0.25, 0.3, 0.4, 0.5, and 1 g/L). Fig. 7 depicts the effect of initial dose of adsorbent on nitrate removal efficiency. It can be seen that the highest nitrate removal efficiency (51%/61%) was obtained in the amount of 0.5 g/L of adsorbent. In this study, with an increase in the absorbent dose, there was no significant increase in nitrate removal efficiency. Therefore, the absorbent dose in nitrate removal is not significant. Lioy et al. [31] reported that nitrate removal rate increases with increasing amount of adsorbent. Similar results were reported by Xing et al. [32].

3.6. Effect of initial concentration of nitrate

The effect of initial concentration of nitrate on removal efficiency is shown in Fig. 8. As seen, with increasing initial concentration of nitrate, removal efficiency was reduced. Hence, with increasing nitrate initial concentration from 25 to 400 mg/L, removal efficiency was decreased from 77%/76% to 28%/83%.

At low concentration of nitrate, specific surface area was high and therefore, adsorption efficiency has been increased. Indeed, by increasing the initial concentration of nitrate, anions amount in competing for replacement in adsorption sites increases and active sites of absorbent are saturated [31]. In the study by Xing et al. [32], reduction in the adsorption of nitrate at high concentrations due to lack of active sites has

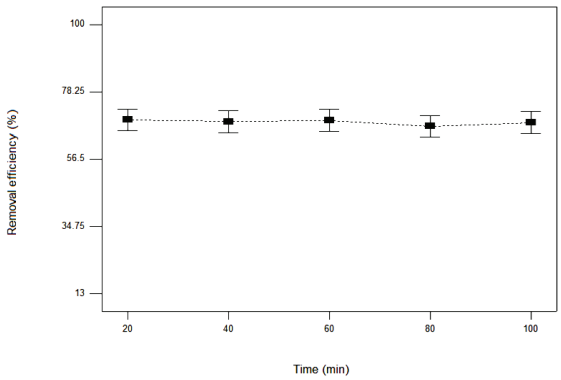

Fig. 4. Effect of contact time on nitrate removal efficiency.

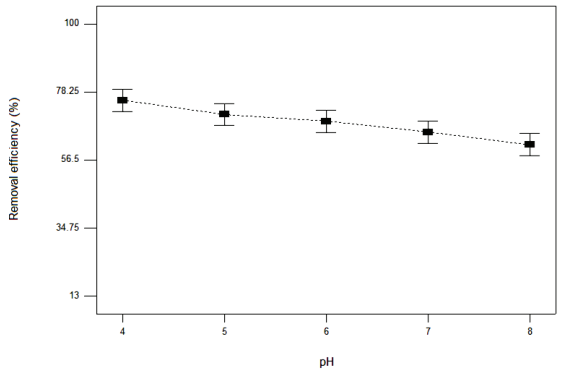

Fig. 5. Effect of pH on nitrate removal efficiency.

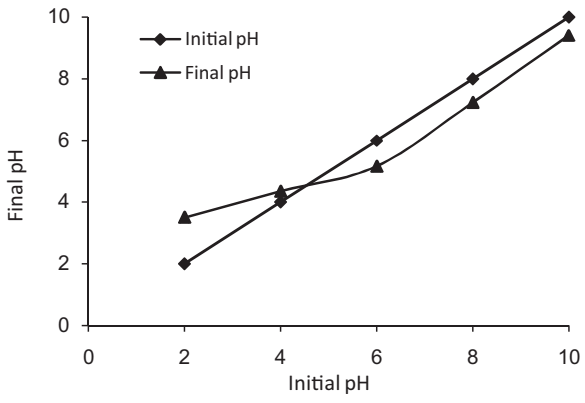

Fig. 6. Determination of adsorbent surface charge.

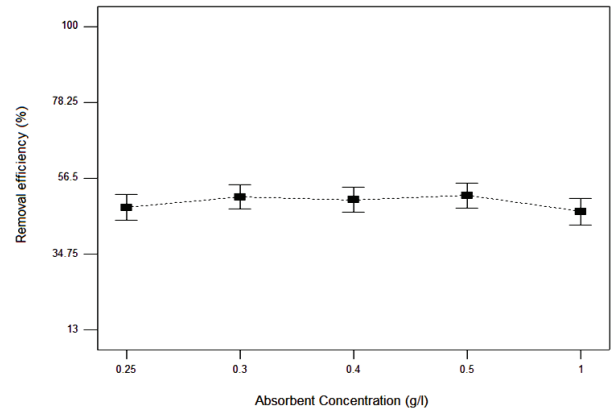

Fig. 7. Effect of absorbent dose on nitrate removal efficiency.

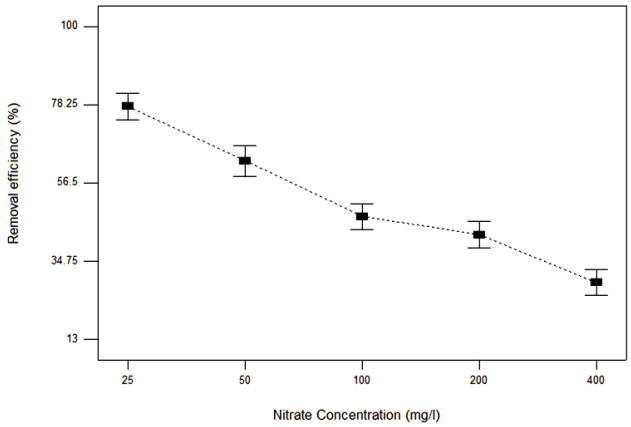

Fig. 8. Effect of nitrate initial concentration on removal efficiency.

been reported. Fernandez-Olmo et al. have reported similar findings as well [33].

The level of significance (P value) was considered 0.05. The significance of the studied model is aimed to explain the adsorption of nitrate ion by synthesized adsorbent and is expressed by F value. This variable was derived 42.68 in the present study and P value was less than 0.05 ($P < 0.0001$). Therefore, the above model is significant for nitrate ion adsorption. In this study, R^2 and adjusted R^2 (R^2_{adj}) were derived 79% and 77%, respectively. The adequate precision value represents the difference between the model's predicted response and the mean predicted error. If this difference exceeds 4, as with the obtained result 24 in the present study, the model is considered appropriate.

A normal distribution diagram was used to confirm the appropriateness of one-way ANOVA. In Fig. 9(a), the studentized residual represents normal distribution, goodness of fit. Ascending diagram of the predicted vs. observed values confirms or rejects the hypothesis of constant variance. The high density of the spots around the diagram represents the constant variance, the correlation among the values, and the distribution of the observed values around regression (Fig. 9(b)). The effects of hidden variables on response variable are investigated by the diagram of residual values vs. the values of the number of experimental steps. Fig. 9(c) illustrates that the data distribution is small and the rate of

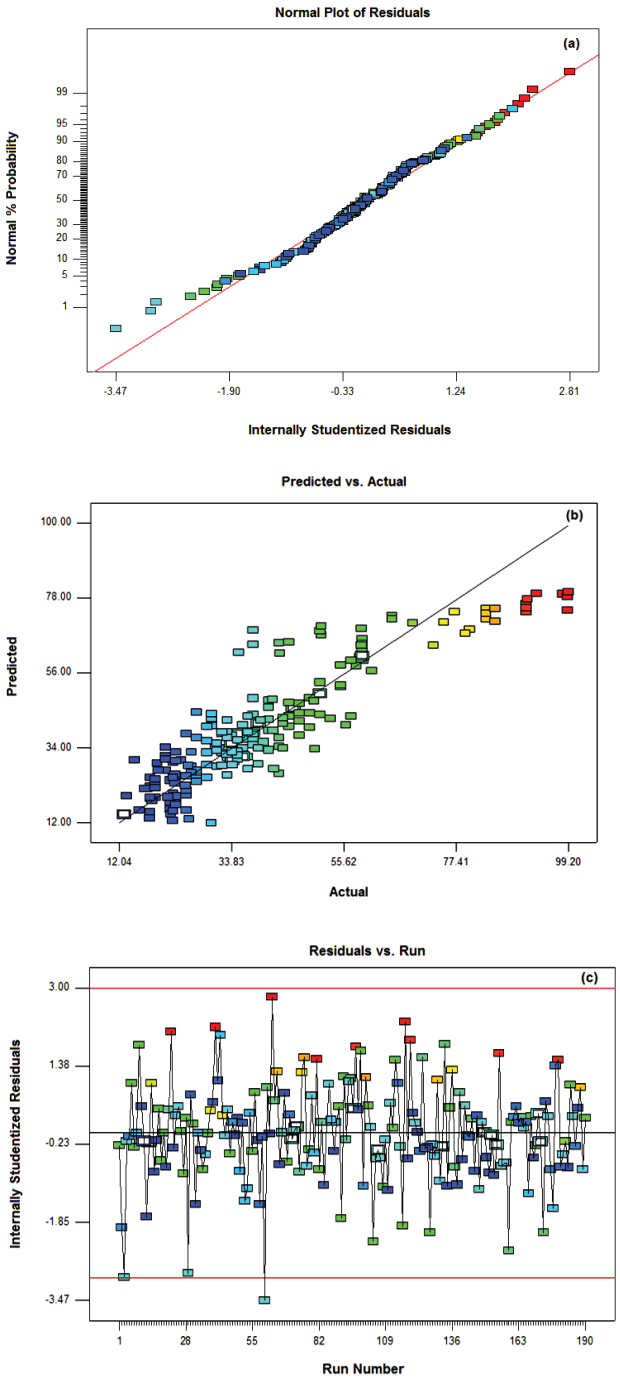

Fig. 9. (a) Normal distribution of residuals, (b) predicted vs. residual values, and (c) residuals vs. run.

constant variance and error percentage is 10% with regard to confidence interval (red lines).

3.7. Adsorption isotherms

In this study, to describe the adsorption equilibrium between the solid and liquid phases, Freundlich and Langmuir isotherm models were used. Linear form of the Freundlich is written as Eq. (3) [9]:

$$\frac{1}{q_e} = \frac{1}{q_m k_L C_e} + \frac{1}{q_m} \quad (3)$$

Linear form of the Freundlich is written as Eq. (4) [9]:

$$\log q_m = \log k_f + \frac{1}{n}\log C_e \quad (4)$$

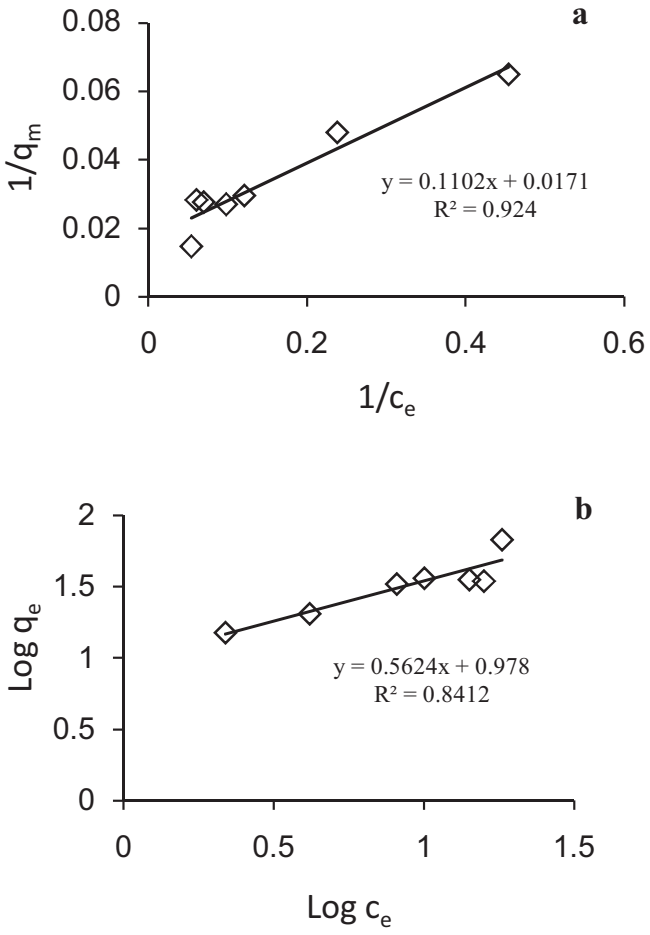

Fig. 10. Langmuir (a) and Freundlich (b) isotherm models on nitrate removal efficiency.

Table 5
Results for Langmuir and Freundlich isotherms parameters

Parameters of Langmuir and Freundlich isotherms				
		q_m (mg/g)	K_L	R^2
Langmuir isotherm model	$\frac{1}{q_e} = \frac{1}{q_m k_L C_e} + \frac{1}{q_m}$	58.47	0.155	0.924
		K	$1/n$	R^2
Freundlich isotherm model	$\log q_m = \log k_f + \frac{1}{n}\log C_e$	9.5	0.5624	0.8412

where q_e (mg/g) is the amount of absorbate per unit mass of absorbent; C_e (mg/g) is the equilibrium concentration of the absorbate in solution after adsorption; q_m and k_L are Langmuir constants obtained from plotting the diagram $1/q_e$ against the diagram $1/C_e$ [9,34] (Fig. 10(a)); and K_f and n are Freundlich constants related to adsorption capacity and intensity obtained from plotting the diagram $\log q_e$ against the diagram $\log C_e$ (Fig. 10(b)).

Comparison of R^2 values showed that the adsorption process matches the Langmuir model due to high R^2 (0.924), this means that the nitrate ion adsorption occurs in certain homogeneous sites and a monolayer adsorption occurs on the surface of the synthesized absorbent. These results are consistent with Hashemian et al. [20]. In this study, the maximum adsorption capacity was obtained equal to 58.47 mg/g. The obtained value of $1/n$ Freundlich models between $0 < 1/n < 1$, which represents the adsorption is desirable. On the other hand, in Langmuir model $R_L = 0.006$ that between 0 and 1, which signifies the optimum adsorption (Table 5).

4. Conclusion

In this study, the possibility of using almond shell activated with magnetic nanoparticles as an absorbent for removal of nitrate ions from aqueous solutions was studied. EDX analysis and FESEM images indicated that absorbent was well activated by magnetic nanoparticles. The conducted studies in this regard demonstrated that solution pH contributed to achieving the maximum removal. The results of experiments on nitrate ions adsorption from aqueous solution using almond shell activated with magnetic nanoparticles showed that, the best conditions for the removal of nitrate were the concentration of 25 mg/L, absorbed dose of 0.5 g/L, the equilibrium time of 20 min and pH 4, with the maximum removal of 79.73%. Also, with increase in the initial concentration of nitrate and absorbent, adsorption decreases and increases, respectively. The mechanism of adsorption process follows Langmuir equation ($R^2 = 0.924$). In view of the results of this study, the removal of nitrate using almond shell activated with magnetic nanoparticles is desirable because of the abundance of almond shell as an agricultural waste, simple system, low cost and high efficiency removal. Magnetic property of the synthesized absorbent makes its isolation from the solution easier after adsorption process, through which an economical, efficient and reliable approach could be accomplished. Hence, almond shell activated with magnetic nanoparticles could be a suitable alternative to the imported, synthetic absorbents currently used.

Acknowledgments

The authors are grateful to Deputy of Research and Technology of Shahrekord University of Medical Sciences (SKUMS) for financial support and laboratory assistance of Department of Environmental Health and Engineering, School of Health, SKUMS. We also thank the National Nanotechnology Development Headquarters to accept and list of this project on the list of nanotechnology.

Competing interests

The authors declare that they have no competing interests.

References

[1] C. Della Rocca, V. Belgiorno, S. Meriç, Overview of in-situ applicable nitrate removal processes, Desalination, 204 (2007) 46–62.

[2] Y. Su, A. Adeleye, Y. Huang, X. Sun, C. Dai, X. Zhou, Y. Zhang, A. Keller, Simultaneous removal of cadmium and nitrate in aqueous media by nanoscale zerovalent iron (nZVI) and Au doped nZVI particles, Water. Res., 63 (2014) 102–111.

[3] P. Ayyasamy, S. Rajakumar, M. Sathishkumar, K. Swaminathan, K. Shanthi, S. Lee, Nitrate removal from synthetic medium and groundwater with aquatic macrophytes, Desalination, 242 (2009) 286–296.

[4] H. Demiral, G. Gündüzoğlu, Removal of nitrate from aqueous solutions by activated carbon prepared from sugar beet bagasse, Bioresour. Technol., 101 (2010) 1675–1680.

[5] S. Chatterjee, D. Lee, M.W. Lee, S. Woo, Nitrate removal from aqueous solutions by cross-linked chitosan beads conditioned with sodium bisulfate, J. Hazard. Mater., 166 (2009) 508–513.

[6] C.H. Liao, S.F. Kang, Y.W. Hsu, Zero-valent iron reduction of nitrate in the presence of ultraviolet light, organic matter and hydrogen peroxide, Water Res., 37 (2003) 4109–4118.

[7] M.H. Ward, T.M. Dekok, P. Levallois, J. Brender, G. Gulis, B.T. Nolan, J. VanDerslice, Workgroup report: drinking-water nitrate and health – recent findings and research needs, Environ. Health Perspect., 113 (2005) 1607–1614.

[8] Institute of Standards and Industrial Research of Iran (ISIRI), Drinking Water: Physical and Chemical Specifications, ISIRI, Tehran, 5th ed., Standard No. 1053, 2009.

[9] S. Chatterjee, S.H. Woo, The removal of nitrate from aqueous solutions by chitosan hydrogel beads, J. Hazard. Mater., 164 (2009) 1012–1018.

[10] A. Bhatnagar, E. Kumar, M. Sillanpää, Nitrate removal from water by nano-alumina: characterization and sorption studies, Chem. Eng., 163 (2010) 317–323.

[11] A. Bhatnagar, M. Sillanpaa, A review of emerging adsorbents for nitrate removal from water, Chem. Eng. J., 168 (2011) 493–504.

[12] M.M. Rao, D.K. Ramana, K. Seshaiah, M.C. Wang, S.W. Chien, Removal of mercury from aqueous solutions using activated carbon prepared from agricultural by-product/waste, J. Environ. Manage., 90 (2009) 634–643.

[13] L.D. Hafshejani, A.R. Hooshmand, A.A. Naseri, A.S. Mohammadi, F. Abbasi, A. Bhatnagar, Removal of nitrate from aqueous solution by modified sugarcane bagasse biochar, Ecol. Eng., 95 (2016) 101–111.

[14] S. Hashemian, A comparative study of cellulose agricultural wastes (almond shell, pistachio shell, walnut shell, tea waste and orange peel) for adsorption of violet B dye from aqueous solutions, Orient. J. Chem., 30 (2014) 2091–2098.

[15] H.Y. Zhu, Y.Q. Fu, R. Jiang, J. Yao, L. Xiao, G.M. Zeng, Novel magnetic chitosan/poly (vinyl alcohol) hydrogel beads: preparation, characterization and application for adsorption of dye from aqueous solution, Bioresour. Technol., 105 (2012) 24–30.

[16] N.M. Nor, L.C. Lau, K.T. Lee, A.D. Mohamed, Synthesis of activated carbon from lignocellulosic biomass and its applications in air pollution control – a review, J. Environ. Chem. Eng., 4 (2013) 658–666.

[17] S. Hashemian, H. Saffari, S. Ragabion, Adsorption of cobalt (II) from aqueous solutions by Fe_3O_4/bentonite nanocomposite, Water Air Soil Pollut., 226 (2015) 2212.

[18] D. Mohan, A. Sarswat, V. Singh, M. Alexandre-Franco, C. Pittman, Development of magnetic activated carbon from almond shells for trinitrophenol removal from water, Chem. Eng. J., 172 (2011) 1111–1125.

[19] K. Mondal, G. Jegadeesan, S.B. Lalvani, Removal of selenate by Fe and NiFe nanosized particles, Ind. Eng. Chem. Res., 43 (2004) 4922–4934.

[20] S. Hashemian, K. Salari, Z.A. Yazdi, Preparation of activated carbon from agricultural wastes (almond shell and orange peel) for adsorption of 2-pic from aqueous solution, J. Ind. Eng. Chem., 20 (2014) 1892–1900.

[21] Y. Bulut, Z. Tez, Adsorption studies on ground shells of hazelnut and almond, J. Hazard. Mater., 149 (2007) 35–41.

[22] R. Bansode, J.N. Losso, W.E. Marshall, R.M. Rao, R.J. Portier, Adsorption of volatile organic compounds by pecan shell- and almond shell-based granular activated carbons, Bioresour. Technol., 90 (2003) 175–184.

[23] K. Thomas Klasson, C.A. Ledbetter, H. Wartelle, S. Lingle, Feasibility of dibromochloropropane (DBCP) and trichloroethylene (TCE) adsorption onto activated carbons made from nut shells of different almond varieties, Ind. Crops Prod., 31 (2010) 261–265.

[24] E. Pehlivan, T. Altun, Biosorption of chromium (VI) ion from aqueous solutions using walnut, hazelnut and almond shell, J. Hazard. Mater., 155 (2008) 378–384.

[25] Q. Hu, N. Chen, C. Feng, W. Hu, Nitrate adsorption from aqueous solution using granular chitosan-Fe^{3+} complex, Appl. Surf. Sci., 347 (2015) 1–9.

[26] P. Janos, H. Buchtova, M. Ryznarova, Sorption of dyes from aqueous solutions onto fly ash, Water. Res., 20 (2003) 4938–4944.

[27] M. Ozmen, K. Can, G. Arslan, A. Tor, Y. Cengeloglu, M. Ersoz, Adsorption of Cu (II) from aqueous solution by using modified Fe_3O_4 magnetic nanoparticles, Desalination, 254 (2010) 162–169.

[28] J. Li, Y. Li, Q. Meng, Removal of nitrate by zero-valent iron and pillared bentonite, J. Hazard. Mater., 174 (2010) 188–193.

[29] M. Seyf-Laye, A. Sika, F. Liu, H. Chen, Optimization of key parameters for chromium (VI) removal from aqueous solutions using activated charcoal, J. Soil Sci. Environ. Manage., 1 (2010) 55–62.

[30] S. Hamoudi, R. Saad, K. Belkacemi, Adsorptive removal of phosphate and nitrate anions from aqueous solutions using ammonium-functionalized mesoporous silica, Ind. Eng. Chem. Res., 46 (2007) 8806–8812.

[31] Y.H. Liou, S.L. Lo, W.H. Kuan, C.J. Lin, S.C. Weng, Effect of precursor concentration on the characteristics of nanoscale zerovalent iron and its reactivity of nitrate, Water Res., 40 (2006) 2485–2492.

[32] X. Xing, B.U. Gao, Q. Zhong, Q. Li, Sorption of nitrate onto amine-crosslinked wheat straw: characteristics, column sorption and desorption properties, J. Hazard. Mater., 186 (2011) 206–211.

[33] I. Fernandez-Olmo, J. Fernandez, A. Irabien, Purification of dilute hydrofluoric acid by commercial ion exchange resins, Sep. Purif. Technol., 56 (2007) 118–125.

[34] G. Nunell, M.E. Fernandez, P.R. Bonelli, A.L. Cukierman, Nitrate uptake improvement by modified activated carbons developed from two species of pine cones, J. Colloid Interface Sci., 440 (2015) 102–108.